Molecular Pharmacology Fast Forward. Published on February 14, 2011 as doi:10.1124/mol.110.068882
This article has not been copyedited and formatted. The final version may differ from this version.

Title Page

Quantitative Analysis Reveals Multiple Mechanisms of Allosteric Modulation of the mGlu5 Receptor in Rat Astroglia

Sophie J. Bradley, Christopher J. Langmead, Jeannette M. Watson and R.A. John Challiss

Department of Cell Physiology and Pharmacology, University of Leicester, Henry Wellcome Building, Lancaster Road, Leicester, LE1 9HN, UK (S.J.B., R.A.J.C.), Heptares Therapeutics Ltd., BioPark, Welwyn Garden City, AL7 3AX, UK (C.J.L), and Neuroscience Centre of Excellence in Drug Discovery, GlaxoSmithKline, New Frontiers Science Park, Harlow, CM19 5AW, UK (J.M.W.)

Molecular Pharmacology Fast Forward. Published on February 14, 2011 as DOI: 10.1124/mol.110.068882
This article has not been copyedited and formatted. The final version may differ from this version.

Running Title Page

Running title: Allosteric modulation of the mGlu5 receptor

Address correspondence to: Dr. R. A. J. Challiss, Department of Cell Physiology and Pharmacology, University of Leicester, Room 4/04, Henry Wellcome Building, Lancaster Road, Leicester, LE1 9HN, U.K. Tel: +44 (0)116 229 7146 - FAX: +44 (0)116 252 5045 - E-mail: jc36@leicester.ac.uk

Manuscript information:

Text Pages	36
Tables	4
Figures	7
Abstract	246 words
Introduction	581 words
Discussion	1500 words
References	40

ABBREVIATIONS: mGlu, metabotropic glutamate; PAM, positive allosteric modulator; NAM, negative allosteric modulator; MPEP, 2-methyl-6-(phenylethynyl)-pyridine; 5MPEP, 5-methyl-2-(phenylethynyl)pyridine; M-5MPEP, 2-(2-(3-methoxyphenyl)ethynyl)-5-methylpyridine; DHPG, (S)-3,5-dihydroxyphenylglycine; ADX47273, S-(4-fluoro-phenyl)-{3-[3-(4-fluoro-phenyl)-[1,2,4]oxadiazol-5-yl]-piperidinl-1-yl}-methanone; DFB, 3,3'-difluorobenzaldazine; CDPPB, 3-cyano-N-(1,3-diphenyl-1H-pyrazol-5-yl)benzamide; CPPHA, N-{4-Chloro-2-[(1,3-dioxo-1,3-dihydro-2H-isoindol-2-yl)methyl]phenyl}-2-hydroxybenzamide; CHO, Chinese hamster ovary; DMEM, Dulbecco's modified Eagle's medium; FBS, fetal bovine serum; [^{3}H]-IP$_x$, [^{3}H]inositol mono, bis- and tris- phosphate fraction.

Molecular Pharmacology Fast Forward. Published on February 14, 2011 as DOI: 10.1124/mol.110.068882
This article has not been copyedited and formatted. The final version may differ from this version.

Abstract

Positive and negative allosteric modulators (PAMs and NAMs, respectively) of the type 5 metabotropic glutamate (mGlu5) receptor have demonstrable therapeutic potential in an array of neurological and psychiatric disorders. Here we have used rat cortical astrocytes to investigate how PAMs and NAMs mediate their activity and reveal marked differences between PAMs with respect to their modulation of orthosteric agonist affinity and efficacy. Affinity cooperativity factors (α) were assessed using [^{3}H]MPEP-PAM competition binding in the absence and presence of orthosteric agonist, while efficacy cooperativity factors (β) were calculated from net affinity/efficacy cooperativity parameters (αβ) obtained from analyses of the abilities of PAMs to potentiate [^{3}H]inositol phosphate accumulation in astrocytes stimulated with a sub-maximal (EC_{20}) concentration of orthosteric agonist. We report that while DFB (3,3'-difluorobenzaldazine) and CDPPB (3-cyano-N-(1,3-diphenyl-1H-prazol-5-yl)benzamide) primarily exert their allosteric modulatory effects through modifying the apparent orthosteric agonist affinity at the astrocyte mGlu5 receptor, the effects of ADX47273 (S-(4-fluoro-phenyl)-{3-[3-(4-fluoro-phenyl)-[1,2,4]oxadiazol-5-yl]-piperidinl-1-yl}-methanone) are mediated primarily via efficacy-driven modulation. In [^{3}H]MPEP-NAM competition binding assays, both MPEP (2-methyl-6-(phenylethynyl)-pyridine) and M-5MPEP (2-(2-(3-methoxyphenyl)ethynyl)-5-methylpyridine) defined similar specific binding components, with affinities that were unaltered in the presence of orthosteric agonist, indicating wholly negative efficacy-driven modulations. Interestingly, while M-5MPEP only partially inhibited orthosteric agonist-stimulated [^{3}H]inositol phosphate accumulation in astrocytes, it could completely suppress Ca^{2+} oscillations stimulated by quisqualate or (*S*)-3,5-dihydroxyphenylglycine. In contrast, MPEP was fully inhibitory with respect to both functional responses. The finding that M-5MPEP has different functional effects depending on the endpoint measured is discussed as a possible example of permissive allosteric antagonism.

Molecular Pharmacology Fast Forward. Published on February 14, 2011 as DOI: 10.1124/mol.110.068882
This article has not been copyedited and formatted. The final version may differ from this version.

Introduction

The major excitatory neurotransmitter glutamate exerts its actions in the central nervous system through binding to two distinct classes of cell-surface receptor; the ionotropic and metabotropic glutamate (mGlu) receptors. The eight mammalian mGlu receptors are family C G protein-coupled receptors, with mGlu1 and mGlu5 receptors constituting the group I sub-family (Conn and Pin, 1997; Niswender and Conn, 2010). Group I mGlu receptors are widely expressed in the mammalian CNS, and in neurons have a predominantly post-synaptic localization. mGlu5 receptors are also expressed in glia, particularly in astrocytes, and the expression of the mGlu5 receptor subtype in astrocytes has been highlighted with respect to a number of potential physiological and pathophysiological roles (Verkhratsky and Kirchhoff, 2007; Wierońska and Pilc, 2009).

Group I mGlu receptors couple via $G\alpha_{q/11}$ proteins to regulate phospholipase C (PLC) activity, as well as mediating G protein-dependent and -independent effects on ion channels and other cellular effector proteins (Hermans and Challiss, 2001; Gerber et al., 2007). Despite sequence, structure and coupling similarities it is generally believed that mGlu1 and mGlu5 receptors subserve distinct functional roles within the brain (Hermans and Challiss, 2001; Bonsi et al., 2008). One consistently reported signal transduction difference between mGlu1 and mGlu5 receptors is the robust Ca^{2+} oscillation initiated by mGlu5, not generally observed following mGlu1 receptor activation (Kawabata et al., 1996; Nakahara et al., 1997; Nash et al., 2001, 2002; Bradley et al., 2009). Work by us and others has provided evidence for the mGlu5 receptor causing Ca^{2+} oscillations via a “dynamic uncoupling” mechanism (Nash et al., 2002), involving a reversible, protein kinase C-dependent phosphorylation of the receptor (at ^{839}Ser; Kim et al., 2005), essentially turning $G_{q/11}$/phospholipase C/Ca^{2+} signaling on and off to create the oscillatory pattern. This unusual mechanism of generating Ca^{2+} oscillations endows this system with specific properties. For example, while changes in mGlu5 receptor expression can alter Ca^{2+} oscillation frequency, this readout is essentially insensitive to changes across the stimulatory concentration range of an orthosteric agonist (e.g. glutamate) (Nash et al., 2002; Bradley et al., 2009). In contrast, allosteric modulation can concentration-dependently increase (positive allosteric modulator; PAM) or decrease (negative allosteric modulator;

Molecular Pharmacology Fast Forward. Published on February 14, 2011 as DOI: 10.1124/mol.110.068882
This article has not been copyedited and formatted. The final version may differ from this version.

NAM) orthosteric agonist-initiated Ca^{2+} oscillation frequency in both recombinant (CHO-*lac*-mGlu5) and native (rat cortical astrocyte) expression systems (Nash et al., 2002; Bradley et al., 2009). Therefore, allosteric modulators can achieve effects beyond the pharmacological repertoire of orthosteric ligands, allowing them to "re-tune" the Ca^{2+} oscillation frequency generated by mGlu5 receptor (orthosteric) occupancy.

An array of molecules have been reported over the past 10 years to interact allosterically with the mGlu5 receptor (Marino and Conn, 2006; Rodriguez and Williams, 2007; Conn et al., 2009); these include NAMs, such as MPEP and M-5MPEP, PAMs, such as DFB, CPPHA, CDPPB and ADX47273, and the neutral allosteric modulator, 5MPEP (Gasparini et al., 1999; O'Brien et al., 2003; O'Brien et al., 2004; Kinney et al., 2005; Rodriguez et al., 2005; Chen et al., 2007; Liu et al., 2008). Positive or negative allosteric modulation of mGlu5 receptor function has been postulated as an approach for the treatment of a number of pathological conditions, including anxiety (Swanson et al., 2005), schizophrenia (Marino and Conn, 2006) and fragile X syndrome (Dölen and Bear, 2008).

Here we have investigated orthosteric/allosteric interactions at the mGlu5 receptor, primarily in rat cortical astrocytes, with a particular objective of applying quantitative pharmacological principles to determine the nature of the agonist/modulator interaction, and also to extend our previous work examining how NAMs and PAMs modulate mGlu5 receptor function at the single cell level.

Molecular Pharmacology Fast Forward. Published on February 14, 2011 as DOI: 10.1124/mol.110.068882
This article has not been copyedited and formatted. The final version may differ from this version.

Materials and Methods

Compounds. Tissue culture reagents, G5 supplement and Fura-2 AM were from Invitrogen (Paisley, UK). *Myo*-[^{3}H]inositol was from GE Healthcare (Chalfont St. Giles, UK). L-quisqualic acid, L-glutamic acid, 2-methyl-6-(phenylethynyl)-pyridine (MPEP), 3,3'-difluorobenzaldazine (DFB) and (S)-3,5-dihydroxyphenylglycine (DHPG) were obtained from Tocris Cookson (Bristol, UK). N-{4-Chloro-2-[(1,3-dioxo-1,3-dihydro-2H-isoindol-2-yl)methyl]phenyl}-2-hydroxybenzamide (CPPHA), 3-cyano-N-(1,3-diphenyl-1H-pyrazol-5-yl)benzamide (CDPPB), S-(4-fluoro-phenyl)-{3-[3-(4-fluoro-phenyl)-[1,2,4]oxadiazol-5-yl]-piperidinl-1-yl}-methanone (ADX47273) and 5-methyl-2-(phenylethynyl)pyridine (5MPEP) were synthesized in-house by GlaxoSmithKline (Harlow, UK). 2-(2-(3-methoxyphenyl)ethynyl)-5-methylpyridine (M-5MPEP) was a kind gift from from Dr. P.J. Conn (Vanderbilt University). [^{3}H]MPEP was from American Radiolabeled Chemicals (Stevenage, UK). All other chemicals and reagents were purchased from Sigma-Aldrich (Poole, Dorset, UK).

Astrocyte preparation and culture. Rat cortical astrocytes were prepared as described previously (Bradley et al., 2009). In brief, neocortices from 2-3 day old Wistar rat pups were subject to proteolysis and dissociation and centrifuged at 1000 r.p.m. for 8 min. Cells were re-suspended into poly-D-lysine-coated T175 tissue culture flasks in Dulbecco's minimum essential medium (DMEM) containing GlutaMAX-1 with sodium pyruvate, 4500 mg L^{-1} glucose, 15% dialyzed fetal bovine serum (FBS), 2.5 μg mL^{-1} amphotericin B, 10^5 U mL^{-1} penicillin, 100 μg mL^{-1} streptomycin. Cell cultures were maintained at 37°C in a humidified 5% CO_2:air atmosphere. Medium was replaced after 3-4 DIV. At 6 DIV medium was replaced and flasks were shaken overnight (320 r.p.m. at 37°C). Following this, confluent cell monolayers were washed twice with PBS (without Ca^{2+}/Mg^{2+}) and harvested with 0.25% (w/v) trypsin, 0.02% (w/v) EDTA. Cells were centrifuged, resuspended in medium (outlined above) and seeded onto poly-D-lysine-coated borosilicate coverslips for imaging experiments or poly-D-lysine-coated 24-well plates for [^{3}H]inositol phosphate experiments. After 24 h,

Molecular Pharmacology Fast Forward. Published on February 14, 2011 as DOI: 10.1124/mol.110.068882
This article has not been copyedited and formatted. The final version may differ from this version.

medium was replaced with medium devoid of fetal bovine serum containing the G5 supplement. Experiments were performed 2-4 days later.

Single-cell intracellular Ca^{2+} concentration ($[Ca^{2+}]_i$) assay. Rat cortical astrocytes were seeded onto 22 mm borosilicate coverslips at 300,000 cells per well and grown to approx. 80% confluency in medium containing G5-supplement. Cells were loaded with Fura-2 AM (2 μM) in KHB containing pluronic acid F127[2] (0.36 mg mL^{-1}) for 45-60 min at room temperature. Coverslips were then transferred to the stage of a Nikon Diaphot inverted epifluorescence microscope, with an oil immersion objective (x40) and a SpectraMASTER II module (PerkinElmer Life Sciences). Cells were excited at wavelengths of 340 and 380 nm using a SpectraMASTER II monochromator and emission was recorded at wavelengths above 520 nm. The ratio of fluorescence intensities at these wavelengths is given as an index of $[Ca^{2+}]_i$. All experiments were performed at 37°C; drug additions were made via a perfusion-line.

Total [^{3}H]-inositol phosphate accumulation assay. Rat cortical astrocytes were seeded at 150,000 cells per well in poly-D-lysine-coated 24-well plates. The following day, cells were incubated in fresh medium containing G5 supplement and 2.5 μCi mL^{-1} [^{3}H]inositol for 48 h. Cell monolayers were washed twice and incubated in Krebs-Henseleit buffer containing GPT (3 U ml^{-1}) and pyruvate (5 mM) for 25 min at 37°C. LiCl (10 mM) was added for a further 20 min prior to agonist incubations for 20 min. Incubations were terminated by aspiration of buffer and rapid addition of 500 μL ice-cold trichloroacetic acid (TCA) (0.5 M). After extraction on ice for 20-30 min samples were transferred to tubes containing 100 μL EDTA (10 mM, pH 7.0) and 500 μL of a 1:1 mixture of tri-*n*-octylamine and 1,1,2-trichlorofluoroethane added. Samples were centrifuged at 14,000 r.p.m. for 2 min and 400 μL of the upper aqueous phase was transferred into fresh tubes containing 100 μL $NaHCO_3$ (62.5 mM). [^{3}H]inositol mono-, bis-, and trisphosphates ([^{3}H]IP_x) were recovered by anion-exchange chromatography on Dowex AG1-X8 formate columns as described previously (Mistry et al., 2005).

Molecular Pharmacology Fast Forward. Published on February 14, 2011 as DOI: 10.1124/mol.110.068882
This article has not been copyedited and formatted. The final version may differ from this version.

Radioligand binding. [^{3}H]MPEP competition binding versus PAMs was conducted as previously described by Liu et al. (2008). In brief, aliquots of membranes (100 μg), prepared from astrocytes or adult rat cortex, were added to tubes containing vehicle or test compounds (final DMSO concentration of 0.33% in all assay tubes) and [^{3}H]MPEP (2 nM final concentration in 50 mM Tris/HCl, 0.9% NaCl, pH 7.4). Tubes were incubated at room temperature for 60 min, with gentle shaking. Membrane-bound ligand was separated from free ligand by rapid filtration onto GF/B glass microfiber filters pre-soaked in wash buffer (20 mM HEPES, 2 mM $CaCl_2$, 2 mM $MgCl_2$, pH 7.2). [^{3}H]MPEP competition binding versus NAMs was conducted as previously described by Anderson et al. (2002). In brief, membranes (100 μg) from astrocytes or adult rat cortex were added to assay buffer (50 mM HEPES, 2mM $MgCl_2$, pH 7.4) containing approx. 10 nM [^{3}H]MPEP and increasing concentrations of each NAM to be studied. Tubes were incubated for 2 h at 4°C. Membrane-bound ligand was separated from free ligand by rapid filtration onto GF/B glass microfiber filters followed by washing twice with ice-cold wash buffer (50 mM Tris/HCl, pH 7.4). In all cases membrane bound radioactivity was extracted overnight and determined by liquid scintillation counting.

Data analysis. Concentration-response relationships were analyzed by non-linear regression using GraphPad Prism 5.0 software (San Diego, CA). Where used, *Equations 3-5* were fitted to mean datasets and estimates of standard error and confidence intervals are from the best-fit parameters.

For [^{3}H]MPEP saturation binding data, the following equation was globally fitted to non-specific and total binding data:

(*Equation 1*)

$$Y = \frac{B_{max} \cdot [A]}{[A] + K_A} + NS \cdot [A]$$

Y is radioligand binding, B_{max} is the total receptor density, [A] is the radioligand concentration, K_A is the equilibrium dissociation constant of the radioligand and NS is the

Molecular Pharmacology Fast Forward. Published on February 14, 2011 as DOI: 10.1124/mol.110.068882
This article has not been copyedited and formatted. The final version may differ from this version.

fraction of non-specific radioligand binding. For radioligand inhibition binding experiments, a one-site binding equation was fitted to the specific binding of each competitive ligand:

(*Equation 2*)

$$Y = Bottom + \frac{(Top - Bottom)}{+ 10^{(Log[B] - LogIC_{50}) \cdot n_H}}$$

where Top and Bottom are the maximal and minimal asymptotes of the curve, respectively, Log [B] is the concentration of inhibitor, log IC_{50} is the logarithm of the concentration of inhibitor that reduces half the maximal radioligand binding for each binding site and n_H is the Hill slope (constrained to unity). IC_{50} values were converted to K_A values (equilibrium dissociation constant) using the Cheng and Prusoff (1973) equation. For the inhibition of [^{3}H]MPEP binding by CPPHA in the presence and absence of quisqualate, the following version of a simple allosteric ternary complex model (Lazareno and Birdsall, 1995) was also fitted to inhibition binding data:

(*Equation 3*)

$$Y = 100 \times \frac{[A]}{\left([A] + \frac{K_A \left(1 + {}^{[B]}/_{K_B} \right)}{\left(1 + {}^{\alpha[B]}/_{K_B} \right)} \right)}$$

Y denotes % specific binding, [A] is the radioligand concentration, K_A is the equilibrium dissociation constant of the radioligand, K_B denotes the allosteric modulator dissociation constant and α denotes the affinity cooperativity factor. Values of $\alpha > 1$ denote positive cooperativity, values $\alpha < 1$ (but greater than 0) denote negative cooperativity and values of 1 denote neutral cooperativity.

Datasets for the positive modulator concentration-response curves in [^{3}H]-IP_X accumulation assays, the quisqualate and modulator titration curves were analyzed globally according to a

Molecular Pharmacology Fast Forward. Published on February 14, 2011 as DOI: 10.1124/mol.110.068882
This article has not been copyedited and formatted. The final version may differ from this version.

modified form of the operational model of allosterism where it is assumed that the orthosteric agonist is full (Leach et al., 2007):

(*Equation 4*)

$$Y = Basal + \frac{(E_M - Basal) \cdot \left(([A](K_B + \alpha\beta[B])) + \tau_B[B] \cdot EC_{50}\right)^n}{(([A](K_B + \alpha\beta[B])) + \tau_B[B] \cdot EC_{50})^n + (EC_{50}{}^n \cdot (K_B[B])^n)}$$

Basal is the response in the absence of ligand, EC_{50} is the midpoint of the full agonist concentration-response curve, K_B is the equilibrium dissociation constant of the allosteric ligand, τ_B denotes the capacity of the allosteric ligand to exhibit agonism (constrained to zero as none of the allosteric modulators exhibit agonist activity) and a $\alpha\beta$ is the net affinity/efficacy cooperativity parameter describing the combined effect of the allosteric modulator on quisqualate function (both affinity and efficacy). The terms E_M and n denote the maximal possible system response and the slope factor of the transducer function that links occupancy to response, respectively.

In order to estimate the degree of affinity cooperativity between quisqualate and the PAMs, inhibition binding curves for PAMs versus [^{3}H]MPEP were determined in the presence and absence of a saturating concentration of quisqualate (30 μM). As total [^{3}H]MPEP binding was unaffected by quisqualate (in the absence of PAMs), the cooperativity between the two ligands must be neutral ($\alpha = 1$). Therefore, to estimate the degree of affinity cooperativity between quisqualate and the PAMs, a ratio of IC_{50} values for each PAM (except CPPHA) in the presence and absence of quisqualate was determined.

NAM inhibition curves for quisqualate and DHPG-stimulated [^{3}H]-IP_X accumulation were analyzed according to a four-parameter logistic equation as described above. For datasets studying the effect of multiple concentrations of NAMs on quisqualate concentration-response curves, data were analyzed according to the full operational model of allosterism (Leach et al., 2007):

Molecular Pharmacology Fast Forward. Published on February 14, 2011 as DOI: 10.1124/mol.110.068882
This article has not been copyedited and formatted. The final version may differ from this version.

(*Equation 5*)

$$Y = Basal + \frac{(E_M - Basal) \cdot ((\tau_A[A](K_B + \alpha\beta[B])) + \tau_B[B] \cdot K_B)^n}{([A]K_B + K_A K_B + K_A[B] + \alpha[A][B])^n + (\tau_A[A](K_B + \alpha\beta[B]) + \tau_B[B] \cdot K_B)^n}$$

This model estimates separately the affinities and efficacies of both orthosteric (K_A, τ_A) and allosteric (K_B, τ_B) ligands as well as the affinity (α) and efficacy (β) cooperativity between the ligand pair. The terms Basal, E_M and n are as described for Equation 4. Estimates of NAM affinities (K_B) were constrained to those generated by [^{3}H]MPEP binding in astrocytes. As quisqualate had no effect on the equilibrium binding of MPEP or M-5MPEP, the affinity cooperativity (α) was constrained to unity. Finally, as the NAMs exhibit no positive agonist activity, τ_B was constrained to zero.

Molecular Pharmacology Fast Forward. Published on February 14, 2011 as DOI: 10.1124/mol.110.068882
This article has not been copyedited and formatted. The final version may differ from this version.

Results

[^{3}H]MPEP binding in astrocyte and cerebrocortical membranes. Saturation analysis of [^{3}H]MPEP binding to membranes prepared from cortical astrocytes treated for 3-4 days with G5 supplement yielded a B_{max} of 667 ± 149 fmol mg^{-1} protein and a K_D value of 2.9 ± 0.5 nM (Fig. 1A). For membranes prepared from adult rat cortex [^{3}H]MPEP saturation binding analysis yielded a B_{max} of 621 ± 27 fmol mg^{-1} protein and a K_D value of 2.1 ± 0.1 nM (Fig. 1B).

Modulation of [^{3}H]MPEP binding by positive allosteric modulators (PAMs). In the presence of a fixed concentration of [^{3}H]MPEP (2 nM), each of the PAMs caused concentration-dependent decreases in [^{3}H]MPEP binding to astrocyte (Fig. 2, left) and cerebrocortical membranes (Fig. 2, right). In astrocyte membranes, ADX47273 caused a similar maximal decrease in [^{3}H]MPEP binding to that seen in the presence of a maximally-effective concentration of MPEP (Fig. 2D, left). CDPPB and DFB caused apparently lesser maximal decreases in specific [^{3}H]MPEP binding (78% and 68% decreases, respectively), likely due to a combination of low affinity and poor solubility (given that previous studies strongly suggest that these PAMs interact with the same binding site as MPEP; O'Brien et al., 2003, 2004; Kinney et al., 2005; Mühlemann et al., 2006). All of the modulators display approx. micromolar affinity for the native mGlu5 receptor (Table 2: *cf.* MPEP pK_i values of 8.03 ± 0.06 and 8.12 ± 0.12 in astrocytes and cortex, respectively).

To assess the effects of agonist occupation of the orthosteric mGlu5 receptor binding site on binding at the [^{3}H]MPEP allosteric site, competition binding studies were repeated in the absence and presence of quisqualate (30 μM) at an orthosteric site-saturating concentration (Mutel et al., 2000). The presence of quisqualate had no effect on total [^{3}H]MPEP binding in membranes prepared from cortical astrocytes or adult rat cortex (1488 ± 27 versus 1507 ± 30 d.p.m. and 1168 ± 112 versus 1211 ± 113 d.p.m in the absence or presence of quisqualate, respectively). However, quisqualate increased the apparent binding affinity of DFB, CDPPB and ADX7273 in both astrocyte and rat cortex membranes (Table 1), causing parallel leftward shifts of the inhibition binding curves to each of these PAMs (Fig. 2A, C, D). The parallel

Molecular Pharmacology Fast Forward. Published on February 14, 2011 as DOI: 10.1124/mol.110.068882
This article has not been copyedited and formatted. The final version may differ from this version.

leftward shifts of the [^{3}H]MPEP-DFB, -CDPPB or -ADX47273 competition curves demonstrate that quisqualate increases the affinity of the PAMs for the mGlu5 receptor. As the concentration of quisqualate used fully occupies mGlu5 receptors (see above), the fold-shift in affinity in the presence and absence of quisqualate represents the degree of affinity cooperativity (termed α) between quisqualate and the respective PAMs. Quisqualate caused a small increase in DFB affinity, which only achieved statistical significance in astrocyte membranes; in contrast, the affinities of both CDPPB and ADX47273 were significantly enhanced in the presence of the agonist, suggesting a high degree of orthosteric-allosteric positive cooperativity (Table 1). It is noteworthy that these cooperativity effects, although evident in rat cortex membranes, were more pronounced in astrocyte preparations. We have also shown that if the orthosteric site is occupied by DHPG (30 μM) or glutamate (300 μM) similar effects are seen on [^{3}H]MPEP versus DFB, CPPHA, CDPPB or ADX47273 interactions to those illustrated here for quisqualate (data not shown) indicating that these modulatory effects are not demonstrably orthosteric probe-dependent.

The profile of CPPHA inhibition of [^{3}H]MPEP binding was markedly different; this PAM caused only an approx. 30% decrease in specific binding in astrocyte membranes (Fig. 2B), while in adult cortex membranes an approx. 50% decrease in specific [^{3}H]MPEP binding was observed. Furthermore, the effect of quisqualate on CPPHA was different to that observed for the other PAMs, causing an increase in the inhibition of specific [^{3}H]MPEP binding (Fig. 2B) without affecting apparent pK_i values (Table 1). These data are consistent with previous observations that CPPHA acts via an allosteric site on the mGlu5 receptor distinct from the MPEP binding site (Chen et al., 2008). Global analysis of the CPPHA inhibition binding isotherms according to a simple ternary complex model (Ehlert, 1988) suggests that CPPHA displays moderate affinity, with pK_B values of 6.16 and 6.15 in astrocytes and cortex, respectively. CPPHA displays weak negative cooperativity with respect to [^{3}H]MPEP binding in astrocytes (α = 0.57) and cortex (α = 0.37), with the degree of negative cooperativity being increased in the presence of quisqualate (α = 0.22 and 0.16 in astrocytes and cortex, respectively).

Molecular Pharmacology Fast Forward. Published on February 14, 2011 as DOI: 10.1124/mol.110.068882
This article has not been copyedited and formatted. The final version may differ from this version.

Effects of positive allosteric modulators on [^{3}H]IP$_x$ responses in astrocytes. To compare the effects of mGlu5 receptor PAMs on orthosteric agonist-stimulated phospholipase C responses in astrocyte populations, we assessed [^{3}H]IP$_x$ accumulation in the presence of Li^+ as an index of PLC activity. None of the mGlu5 receptor PAMs studied here (DFB, CPPHA, CDPPB, ADX47273) increased [^{3}H]IP$_x$ accumulation over basal levels when added alone to astrocytes (data not shown). Therefore, the ability of PAMs to increase [^{3}H]IP$_x$ accumulation was assessed in the presence of 50 nM quisqualate, a concentration which alone causes a [^{3}H]IP$_x$ response that is ~20% (EC_{20}) of the maximal quisqualate response (Fig. 3). CDPPB and ADX47273 were each able to potentiate [^{3}H]IP$_x$ accumulation stimulated by 50 nM quisqualate to a level comparable to that seen in the presence of a maximally-effective concentration of quisqualate alone. In contrast, in the presence of DFB or CPPHA less potentiation was observed (approx. 10% and 65% of maximum quisqualate response, respectively). Therefore, the efficacy rank-order for these PAMs was: ADX47273 ≈ CDPPB > CPPHA > DFB; whereas the potency rank-order was CDPPB > CPPHA ≥ ADX47273 ≥ DFB (see Table 2).

In order to further understand PAM effects, the modulator concentration-response curves were analyzed according to a modified form of the operational model of allosterism (Leach et al., 2007; *Equation 4* in Methods) to yield an estimate of modulator affinity (pK_B) and overall cooperativity with respect to quisqualate ($\alpha\beta$; comprising any effects on affinity and/or efficacy). Parameter estimates are shown in Table 2. The affinity rank-order was identical to that seen for the EC_{50} values of the PAMs, whereas the estimate of cooperativity ($\alpha\beta$) correlated to the potentiation (fold-increase) of the EC_{20} quisqualate response (Table 2).

Quantification of the effects of the PAMs on the quisqualate [^{3}H]IP$_x$ accumulation response yields estimates of the overall degree of cooperativity between the respective PAMs and quisqualate (a product of the effect on affinity and efficacy, $\alpha\beta$). Using the value for affinity cooperativity (α) derived from the [^{3}H]MPEP binding studies, it is possible to estimate the efficacy cooperativity between each of the PAMs (except CPPHA) and quisqualate (Table 2). These data suggest that DFB exerts its modest positive modulatory effect through marginal effects on affinity and efficacy (α = 1.5, β = 1.4). Importantly, despite qualitatively similar

Molecular Pharmacology Fast Forward. Published on February 14, 2011 as DOI: 10.1124/mol.110.068882
This article has not been copyedited and formatted. The final version may differ from this version.

effects on quisqualate-stimulated [^{3}H]IP$_x$ accumulation, quantitative analysis reveals that CDPPB and ADX47273 achieve their positive modulation in different ways. The modulatory effect of CDPPB is largely achieved by an increase in quisqualate affinity, with only a modest effect on efficacy (α = 11, β = 2.3), whereas ADX47273 exerts its effects mainly through increases in quisqualate efficacy, with a more modest effect on affinity (α = 3.2, β = 9.4).

Negative allosteric modulator (NAM) affinity estimates at mGlu5 receptors. mGlu5 receptor binding affinities for MPEP and M-5MPEP were determined by competition analysis of [^{3}H]MPEP binding to astrocyte (Fig. 4A; Table 3) and rat cortex membranes (Fig. 4B; Table 3). Both negative allosteric modulators defined similar non-specific binding components for [^{3}H]MPEP binding to astrocyte and rat cortex membranes: pK$_i$ values obtained in the two membrane preparations revealed that M-5MPEP and the neutral allosteric site compound, 5MPEP (data not shown), are equi-effective in displacing [^{3}H]MPEP binding and both compounds are 30-100 fold less potent compared to MPEP (Table 3). To assess the effects of orthosteric site occupation, adult rat cortex membranes were incubated with a high (30 μM) concentration of quisqualate and [^{3}H]MPEP versus MPEP or M-5MPEP competition analyses performed (Fig. 4C-D; Table 3). Agonist occupation of the orthosteric site had no effect on the interaction between negative/neutral allosteric modulators and [^{3}H]MPEP. These data suggest that unlike the PAMs, the NAMs exhibit neutral affinity cooperativity with respect to quisqualate (α = 1). The above findings were wholly recapitulated if studies were repeated under the assay conditions of Liu et al. (2008) used for the [3H]MPEP-PAM radioligand studies (data not shown).

Effects of NAMs on astrocyte single-cell Ca^{2+} responses. The NAM, MPEP has previously been shown to decrease glutamate-stimulated Ca^{2+} oscillations in a concentration-dependent manner in CHO-*lac*-mGlu5a cells and astrocytes (Nash et al., 2002; Bradley et al., 2009). Here, we have extended these previous studies to include a comparison between MPEP and the "partial" NAM M-5MPEP (Rodriguez et al., 2005), and also to investigate whether any probe-dependency is observed by assessing the effects of these NAMs on Ca^{2+} oscillations initiated by quisqualate, DHPG or glutamate. Although, the frequency of Ca^{2+} oscillations stimulated by each of these orthosteric agonists varied slightly, the concentration-dependency

Molecular Pharmacology Fast Forward. Published on February 14, 2011 as DOI: 10.1124/mol.110.068882
This article has not been copyedited and formatted. The final version may differ from this version.

for MPEP-induced suppressions of agonist-stimulated responses did not appear to be probe-dependent, giving a $pIC_{50} \approx 8$ and full inhibition versus each of the orthosteric agonists tested (Fig. 5; Table 4). M-5MPEP also caused concentration-dependent, probe-independent, full inhibition of orthosteric agonist-stimulated Ca^{2+} oscillations in astrocytes (Fig. 6; Table 4), observations in agreement with results obtained previously in CHO-*lac*-mGlu5a cells (Bradley et al., 2009). Given that the affinity cooperativity between the NAMs and quisqualate is neutral, the inhibitory effects of the NAMs must be mediated by a change in agonist efficacy. Although it was not possible to quantify the degree of efficacy cooperativity between NAMs and quisqualate (as the data are only for a single curve), the full inhibition of agonist-stimulated Ca^{2+} oscillations suggests that the value of β must tend towards zero.

Effects of NAMs on phosphoinositide hydrolysis in astrocytes. In the presence of Li^+, addition of quisqualate for 20 min stimulated an approx. 6-fold increase in $[^3H]IP_x$ accumulation (basal, 74,899 ± 1389; +quisqualate (30 μM), 447,086 ± 16090 d.p.m. mg^{-1} protein: pEC_{50} (M) = 6.80 ± 0.02). The mGlu5 receptor NAMs, MPEP and M-5MPEP, decreased the $[^3H]IP_x$ accumulation stimulated by quisqualate (10 μM) in a concentration-dependent manner (Fig. 7; Table 4), whereas 5-MPEP was without effect (data not shown). The pIC_{50} values for MPEP-mediated inhibition of mGlu5 receptor-mediated $[^3H]IP_x$ accumulation compared well with pIC_{50} values derived for the inhibition of Ca^{2+} oscillations (Table 4); whereas lower IC_{50} values were observed for inhibitory effects on Ca^{2+} oscillations relative to $[^3H]IP_x$ accumulation for M-5MPEP (Table 4). More strikingly, whereas MPEP was able to inhibit fully agonist-stimulated $[^3H]IP_x$ accumulation, M-5MPEP only partially inhibited this response (Fig. 7A, B), contrasting with the ability of this NAM to inhibit completely the Ca^{2+} response. This "partial NAM" effect of M-5MPEP was also observed with respect to the $[^3H]IP_x$ accumulation stimulated by DHPG (Fig. 7B). Using an alternative experimental design, it could be shown that increasing concentrations of MPEP progressively suppress quisqualate-stimulated $[^3H]IP_x$ accumulation in astrocytes with only a approx. 3-fold change in apparent quisqualate potency (Fig. 7C; pEC_{50} (M): -MPEP, 6.72 ± 0.09; +1 μM MPEP, 6.24 ± 0.11). Qualitatively the effect of MPEP is highly likely to be mediated by changes in quisqualate efficacy, as the ligands exhibit neutral affinity cooperativity with respect to one another (see above). Analysis of the dataset according to the operational model

Molecular Pharmacology Fast Forward. Published on February 14, 2011 as DOI: 10.1124/mol.110.068882
This article has not been copyedited and formatted. The final version may differ from this version.

of allosterism (Leach et al., 2007; *Equation 5* in Methods), indicates a high degree of negative efficacy cooperativity between quisqualate and MPEP ($\beta = 0.01$), reflecting the full inhibition of quisqualate-stimulated [^{3}H]IP$_x$ accumulation. These data are quantitatively similar to those seen for MPEP in the Ca^{2+} oscillation assay. In contrast, increasing concentrations of M-5MPEP (up to 30 μM) resulted in only a partial, concentration-dependent suppression of quisqualate-stimulated [^{3}H]IP$_x$ accumulation (Fig. 7D). Quantitative analysis of the interaction between M-5MPEP and quisqualate suggests a weak degree of negative efficacy cooperativity ($\beta = 0.37$) between the two ligands in the [^{3}H]IP$_x$ accumulation assay, in marked contrast to the full inhibitory effect (β approaches zero) observed in the Ca^{2+} oscillation assay.

Molecular Pharmacology Fast Forward. Published on February 14, 2011 as DOI: 10.1124/mol.110.068882
This article has not been copyedited and formatted. The final version may differ from this version.

Discussion

The discovery of compounds that alter mGlu receptor activity through binding to allosteric sites within the transmembrane domain has been rapidly followed-up by the generation of an array of compounds that show good mGlu receptor subtype selectivity, as well as additional pharmacologically desirable pharmacokinetic/pharmacodynamic properties (Conn et al., 2009; Niswender and Conn, 2010). Positive or negative allosteric modulation of the mGlu5 receptor has been indicated as a fruitful therapeutic approach in a number of neuro-psychiatric disorders (Swanson et al., 2005; Marino and Conn, 2006; Dölen and Bear, 2008). While mGlu5 receptor PAMs and NAMs can exert direct agonist or inverse agonist activity, for example, at a mutant mGlu5 receptor where the *N*-terminal orthosteric ligand binding domain has been removed (Goudet et al., 2004), the majority of the NAMs and PAMs reported to date (and those investigated here) are considered to be true modulators in that they alter the ability of orthosteric agonists to effect mGlu5 receptor activity. This allosteric modulatory action can be brought about by altering the affinity and/or the efficacy of the orthosteric agonist at the receptor (Langmead and Christopoulos, 2006). Surprisingly, little information is currently available defining the mode of mGlu5 receptor allosteric modulation and a key objective of the present study has been to provide a more quantitative analysis of the actions of prototypic NAMs and PAMs at native mGlu5 receptors.

To achieve this we first examined the interaction of NAMs and PAMs at the MPEP site on the mGlu5 receptor utilizing [^{3}H]MPEP binding. The density of [^{3}H]MPEP binding sites in G5 supplement-differentiated rat cortical astrocytes approximated that found in adult rat cerebral cortex, however it should be noted that the major splice variant expressed in the former is the mGlu5a (Biber et al., 1999), while mGlu5b is likely to predominate in the latter (Minakami et al., 1995). The NAMs MPEP and M-5MPEP, and the neutral allosteric modulator 5-MPEP, all competed for the [^{3}H]MPEP binding site in membrane preparations from rat cortical astrocytes and cerebral cortex and defined identical levels of specific binding. Competition isotherms were completely unaffected by the absence or presence of quisqualate at a concentration expected to occupy fully the orthosteric binding site. In contrast, PAMs

Molecular Pharmacology Fast Forward. Published on February 14, 2011 as DOI: 10.1124/mol.110.068882
This article has not been copyedited and formatted. The final version may differ from this version.

inhibited [^{3}H]MPEP binding to different extents. Previous work has demonstrated that DFB (O'Brien et al., 2003), CDPPB (Kinney et al., 2005; Chen et al., 2007) and ADX47273 (Liu et al., 2006) bind to a similar (or substantially overlapping) allosteric binding site to MPEP, whereas CPPHA binds to a distinct locus within the mGlu5 receptor 7-transmembrane domain (O'Brien et al., 2004; Chen et al., 2008). Indeed, a number of studies have provided information on the amino acid residues that contribute to common NAM/PAM-mGlu5 receptor interactions (Gasparini et al., 1999; Mühlemann et al., 2006). While apparently incomplete inhibition of specific [^{3}H]MPEP binding has been observed previously for DFB (versus the MPEP analog [^{3}H]methoxyPEPy; O'Brien et al., 2003); another study has reported that high concentrations of CDPPB can inhibit [^{3}H]methoxyPEPy binding to similar levels to MPEP (Kinney et al., 2005). Therefore, although it might be tempting to speculate on possible allosteric interactions of these PAMs with respect to [^{3}H]MPEP binding it is more likely that technical difficulties (e.g. low affinity, compound solubility problems, etc.) underlie the [^{3}H]MPEP competition binding isotherms observed for DFB and CDPPB. Notwithstanding these concerns, it is clear that agonist-occupancy of the mGlu5 orthosteric binding site alters the apparent affinity of DFB, CDPPB and ADX47273 at the [^{3}H]MPEP binding site, with respective 1.5, 3.2 and 11-fold leftward shifts (α values) being seen in astrocyte membranes. In contrast, agonist occupancy of the orthosteric site did not affect the apparent affinity of CPPHA for the [^{3}H]MPEP binding site, but analysis using the allosteric ternary complex model revealed the degree to which negative cooperativity was increased. These latter data confirm and extend previous studies on the pharmacological properties of CPPHA (O'Brien et al., 2004; Chen et al., 2008).

To investigate efficacy-related effects of PAMs we adopted a protocol utilized previously (O'Brien et al., 2003, 2004; Kinney et al., 2005; Chen et al., 2008; Liu et al., 2008), however, [^{3}H]IP_x accumulation rather than a population Ca^{2+} response was used here as a readout. Quisqualate stimulated a ~6 fold increase in [^{3}H]IP_x accumulation in astrocytes in the presence of Li^+. In the presence of an approx. EC_{20} concentration (50 nM) of the orthosteric agonist each of the PAMs caused an enhancement of the quisqualate-stimulated [^{3}H]IP_x accumulation, but to different extents. Qualitatively the maximal response ranking order was ADX47273 ≈ CDPPB > CPPHA > DFB with maximal potentiation of the 50 nM quisqualate

response varying from 4.7 fold down to 1.5 fold. Further analysis using a modified form of the operational model of allosterism (Leach et al., 2007 – see *Methods*) yielded net affinity/efficacy cooperativity parameters (αβ – Table 2), which varied from 30 (ADX47273) to 2.1 (DFB). By utilizing the previously determined affinity cooperativity (α) parameters, it was possible to resolve affinity and efficacy components for each PAM. Strikingly, we have demonstrated that ADX47273 and CDPPB differ substantially in the ways that they exert their PAM actions. Whereas CDPPB is primarily an *affinity* modulator (i.e. exerts it PAM activity through increasing the apparent mGlu5 receptor binding affinity for orthosteric agonists), ADX47273 exerts a much greater part of its PAM activity through *efficacy* modulation. Thus, through the application of quantitative pharmacological analyses it is possible to reveal marked mechanistic differences between allosteric modulators that are not apparent from more conventional analysis. That two PAMs bind to a common site to exert mechanistically different allosteric effects is not inconsistent with our current understanding of allostery at GPCRs (Kenakin and Miller, 2010). Indeed, it would be interesting to perform mutagenesis studies to establish whether, within the mGlu5 receptor MPEP binding pocket, the amino acid residues critical for the actions of each PAM diverge and thus provide an empirical basis for the differing receptor ensemble conformational selectivity of the two PAMs that might be hypothesized. These new findings also raise the issue of whether the mechanism of positive allosteric modulation is of potential importance from a therapeutic perspective, *i.e.* with respect to the therapeutic deployment of mGlu5 receptor PAMs in neuro-psychiatric disorders is an affinity- or efficacy-driven modulation more desirable?

Competition analyses for MPEP and M-5MPEP versus [^{3}H]MPEP binding in astrocyte and adult cerebral cortex membranes indicated similar definitions of specific (displaceable) binding and a complete lack of effect of agonist occupation of the orthosteric site on respective competition isotherms, strongly indicating that these agents exert their negative modulatory activity through efficacy rather than affinity effects. A mechanism for efficacy-only modulation is unclear and these effects could be mediated via changes in receptor-G protein interaction. The effects of the NAMs are unlikely to be due to steric hindrance between G protein and receptor as previous site-directed mutagenesis studies have clearly indicated a transmembrane domain binding locus. Therefore, it could be that there is negative

Molecular Pharmacology Fast Forward. Published on February 14, 2011 as DOI: 10.1124/mol.110.068882
This article has not been copyedited and formatted. The final version may differ from this version.

affinity cooperativity between the G protein and NAM, but not between orthosteric agonist(s) and the NAM. This manifests as apparent 'negative efficacy cooperativity' when considering only the ternary complex of orthosteric agonist, receptor and NAM. However, it is possible to argue that if a quaternary complex, incorporating G protein, is considered then the differential affinity cooperativity of PAMs and NAMs (with either orthosteric agonist or G protein) might become apparent; however, the necessary tools are not presently available to test this possibility.

To further compare MPEP and M-5MPEP, we assessed their respective abilities to inhibit orthosteric agonist-stimulated $[^3H]IP_x$ accumulation and single cell Ca^{2+} oscillations in astrocytes. While MPEP fully inhibited both functional responses with pIC_{50} values consistent with previous studies (Gasparini et al., 1999; Nash et al., 2002; O'Brien et al., 2003; Rodriguez et al., 2005; Chen et al., 2008), M-5MPEP only partially inhibited the $[^3H]IP_x$ response (irrespective of whether it was stimulated by quisqualate or DHPG), but fully inhibited Ca^{2+} oscillations stimulated by L-glutamate, quisqualate or DHPG. In the original report on M-5MPEP this compound was described as a "partial antagonist" based on its ability only partially to inhibit glutamate-stimulated changes in $[Ca^{2+}]_i$ in populations of astrocytes (Rodriguez et al., 2005). Here we have reproduced this original finding with respect to the $[^3H]IP_x$ response, but, as reported previously in CHO-*lac*-mGlu5a cells (Bradley et al., 2009), M-5MPEP also appears to possess a greater inverse efficacy with respect to Ca^{2+} oscillatory responses in astrocytes. It is also noteworthy that the potency of M-5MPEP for the inhibition of Ca^{2+} oscillations was significantly greater than for the (partial) inhibition of $[^3H]IP_x$ accumulation. For example, M-5MPEP displayed a 17 fold greater potency for inhibiting quisqualate-stimulated Ca^{2+} oscillations versus $[^3H]IP_x$ responses. As discussed previously mGlu5 receptor-mediated Ca^{2+} oscillations are driven by phosphorylation/dephosphorylation of the receptor itself (Nash et al., 2002; Bradley et al., 2009) driven by diacylglycerol (and Ca^{2+}) -dependent protein kinase C isoenzymes. Therefore, while it is difficult to view the $[^3H]IP_x$ and Ca^{2+} oscillatory responses as independent readouts, it is nevertheless tempting to speculate that M-5MPEP may be a NAM that can display permissive antagonism (Kenakin, 2005).

Molecular Pharmacology Fast Forward. Published on February 14, 2011 as DOI: 10.1124/mol.110.068882
This article has not been copyedited and formatted. The final version may differ from this version.

Acknowledgements

We thank the Biotechnology and Biological Sciences Research Council of Great Britain for the award of a PhD CASE studentship to S.J.B.

Molecular Pharmacology Fast Forward. Published on February 14, 2011 as DOI: 10.1124/mol.110.068882
This article has not been copyedited and formatted. The final version may differ from this version.

Author Contributions

Participated in research design: Bradley, Langmead, Watson, and Challiss

Conducted experiments: Bradley

Performed data analysis: Bradley, Langmead, and Challiss

Wrote or contributed to the writing of the manuscript: Bradley, Langmead, and Challiss

Molecular Pharmacology Fast Forward. Published on February 14, 2011 as DOI: 10.1124/mol.110.068882
This article has not been copyedited and formatted. The final version may differ from this version.

References

Anderson JJ, Rao SP, Rowe B, Giracello DR, Holtz G, Chapman DF, Tehrani L, Bradbury MJ, Cosford ND, and Varney MA (2002) [^{3}H]Methoxymethyl-3-[(2-methyl-1,3-thiazol-4-yl)ethynyl]pyridine binding to metabotropic glutamate receptor subtype 5 in rodent brain: in vitro and in vivo characterization. *J Pharmacol Exp Ther* **303:**1044-1051.

Biber K, Laurie DJ, Berthele A, Sommer B, Tölle TR, Gebicke-Härter PJ, van Calker D, Boddeke HWGM (1999) Expression and signaling of group I metabotropic glutamate receptors in astrocytes and microglia. *J Neurochem* **72:**1671-1680.

Bonsi P, Platania P, Martella G, Madeo G, Vita D, Tassone A, Bernardi G, and Pisani A (2008) Distinct roles of group I mGlu receptors in striatal function. *Neuropharmacology* **55:**392-395.

Bradley SJ, Watson JM, and Challiss RAJ (2009) Effects of positive allosteric modulators on single-cell oscillatory Ca^{2+} signaling initiated by the type 5 metabotropic glutamate receptor. *Mol Pharmacol* **76:**1302-1313.

Chen Y, Goudet C, Pin JP, and Conn PJ (2008) N-{4-Chloro-2-[(1,3-dioxo-1,3-dihydro-2H-isoindol-2-yl)methyl]phenyl}-2-hydroxybenzamide (CPPHA) acts through a novel site as a positive allosteric modulator of group 1 metabotropic glutamate receptors. *Mol Pharmacol* **73:**909-918.

Chen Y, Nong Y, Goudet C, Hemstapat K, de Paulis T, Pin JP, and Conn PJ (2007) Interaction of novel positive allosteric modulators of metabotropic glutamate receptor 5 with the negative allosteric antagonist site is required for potentiation of receptor responses. *Mol Pharmacol* **71:**1389-1398.

Cheng Y and Prusoff WH (1973) Relationship between the inhibition constant (K_i) and the concentration of inhibitor which causes 50 per cent inhibition (I_{50}) of an enzymatic reaction. *Biochem Pharmacol* **22:**3099-3108.

Conn PJ and Pin JP (1997) Pharmacology and functions of metabotropic glutamate receptors. *Annu Rev Pharmacol Toxicol* **37:**205-237.

Conn PJ, Christopoulos A, and Lindsley CW (2009) Allosteric modulators of GPCRs: a novel approach for the treatment of CNS disorders. *Nat Rev Drug Discov* **8:**41-54.

Dölen G and Bear MF (2008) Role for metabotropic glutamate receptor 5 (mGluR5) in the pathogenesis of fragile X syndrome. *J Physiol* **586:**1503-1508.

Ehlert FJ (1988) Estimation of the affinities of allosteric ligands using radioligand binding and pharmacological null methods. *Mol Pharmacol* **33:**187-194.

Gasparini F, Lingenhöhl K, Stoehr N, Flor PJ, Heinrich M, Vranesic I, Biollaz M, Allgeier H, Heckendorn R, Urwyler S, et al. (1999) 2-Methyl-6-(phenylethynyl)-pyridine (MPEP), a potent, selective and systemically active mGlu5 receptor antagonist. *Neuropharmacology* **38:**1493-1503.

Gerber U, Gee CE, and Benquet P (2007) Metabotropic glutamate receptors: intracellular signaling pathways. *Curr Opin Pharmacol* **7:**56-61.

Goudet C, Gaven F, Kniazeff J, Vol C, Liu J, Cohen-Gonsaud M, Acher F, Prézeau L, and Pin JP (2004) Heptahelical domain of metabotropic glutamate receptor 5 behaves like rhodopsin-like receptors. *Proc Natl Acad Sci USA* **101:**378-383.

Hermans E and Challiss RAJ (2001) Structural, signalling and regulatory properties of the group I metabotropic glutamate receptors: prototypic family C G-protein-coupled receptors. *Biochem J* **359:**465-484.

Kawabata S, Tsutsumi R, Kohara A, Yamaguchi T, Nakanishi S, and Okada M (1996) Control of calcium oscillations by phosphorylation of metabotropic glutamate receptors. *Nature* **383:**89-92.

Kenakin T (2005) New concepts in drug discovery: collateral efficacy and permissive antagonism. *Nat Rev Drug Discov* **4:**919-927.

Kenakin T and Miller LJ (2010) Seven transmembrane receptors as shapeshifting proteins: the impact of allosteric modulation and functional selectivity on new drug discovery. *Pharmacol Rev* **62:**265-304.

Kim CH, Braud S, Isaac JT, and Roche KW (2005) Protein kinase C phosphorylation of the metabotropic glutamate receptor mGluR5 on serine-839 regulates Ca^{2+} oscillations. *J Biol Chem* **280:**25409-25415.

Kinney GG, O'Brien JA, Lemaire W, Burno M, Bickel DJ, Clements MK, Chen TB, Wisnoski DD, Lindsley CW, Tiller PR, et al. (2005) A novel selective positive allosteric modulator of metabotropic glutamate receptor subtype 5 has in vivo activity and antipsychotic-like effects in rat behavioral models. *J Pharmacol Exp Ther* **313:**199-206.

Langmead CJ and Christopoulos A (2006) Allosteric agonists of 7TM receptors: expanding the pharmacological toolbox. *Trends Pharmacol Sci* **27:**475-481.

Lazareno S and Birdsall NJM (1995) Detection, quantitation, and verification of allosteric interactions of agents with labeled and unlabeled ligands at G protein-coupled receptors: interactions of strychnine and acetylcholine at muscarinic receptors. *Mol Pharmacol* **48:**362-378.

Leach K, Sexton PM, and Christopoulos A (2007) Allosteric GPCR modulators: taking advantage of permissive receptor pharmacology. *Trends Pharmacol Sci* **28:**382-389.

Liu F, Grauer S, Kelley C, Navarra R, Graf R, Zhang G, Atkinson PJ, Popiolek M, Wantuch C, Khawaja X, et al. (2008) ADX47273 [S-(4-fluoro-phenyl)-{3-[3-(4-fluoro-phenyl)-[1,2,4]-oxadiazol-5-yl]-piperidin-1-yl}-methanone]: a novel metabotropic glutamate receptor 5-selective positive allosteric modulator with preclinical antipsychotic-like and precognitive activities. *J Pharmacol Exp Ther* **327:**827-839.

Marino MJ and Conn PJ (2006) Glutamate-based therapeutic approaches: allosteric modulators of metabotropic glutamate receptors. *Curr Opin Pharmacol* **6:**98-102.

Minakami R, Iida K, Hirakawa N, and Sugiyama H (1995) The expression of two splice variants of metabotropic glutamate receptor subtype 5 in the rat brain and neuronal cells during development. *J Neurochem* **65:**1536-1542.

Mistry R, Dowling MR, and Challiss RAJ (2005) An investigation of whether agonist-selective receptor conformations occur with respect to M_2 and M_4 muscarinic acetylcholine receptor signalling via $G_{i/o}$ and G_s proteins. *Br J Pharmacol* **144:**566-575.

Mühlemann A, Ward NA, Kratochwil N, Diener C, Fischer C, Stucki A, Jaeschke G, Malherbe P, and Porter RH (2006) Determination of key amino acids implicated in the actions of allosteric modulation by 3,3'-difluorobenzaldazine on rat mGlu5 receptors. *Eur J Pharmacol* **529:**95-104.

Mutel V, Ellis GJ, Adam G, Chaboz S, Nilly A, Messer J, Bleuel Z, Metzler V, Malherbe P, Schlaeger EJ, et al. (2000) Characterization of [^{3}H]quisqualate binding to recombinant rat metabotropic glutamate 1a and 5a receptors and to rat and human brain sections. *J Neurochem* **75:**2590-2601.

Nakahara K, Okada M, and Nakanishi S (1997) The metabotropic glutamate receptor mGluR5 induces calcium oscillations in cultured astrocytes via protein kinase C phosphorylation. *J Neurochem* **69:**1467-1475.

Nash MS, Schell MJ, Atkinson PJ, Johnston NR, Nahorski SR, and Challiss RAJ (2002) Determinants of metabotropic glutamate receptor-5-mediated Ca^{2+} and inositol 1,4,5-trisphosphate oscillation frequency. *J Biol Chem* **277:**35947-35960.

Nash MS, Young KW, Challiss RAJ, and Nahorski SR (2001) Intracellular signalling. Receptor-specific messenger oscillations. *Nature* **413:**381-382.

Niswender CM and Conn PJ (2010) Metabotropic glutamate receptors: physiology, pharmacology, and disease. *Annu Rev Pharmacol Toxicol* **50:**295-322.

O'Brien JA, Lemaire W, Chen TB, Chang RS, Jacobson MA, Ha SN, Lindsley CW, Schaffhauser HJ, Sur C, Pettibone DJ, et al. (2003) A family of highly selective allosteric modulators of the metabotropic glutamate receptor subtype 5. *Mol Pharmacol* **64:**731-740.

O'Brien JA, Lemaire W, Wittmann M, Jacobson MA, Ha SN, Wisnoski DD, Lindsley CW, Schaffhauser HJ, Rowe B, Sur C, et al. (2004) A novel selective allosteric modulator potentiates the activity of native metabotropic glutamate receptor subtype 5 in rat forebrain. *J Pharmacol Exp Ther* **309:**568-577.

Rodriguez AL, Nong Y, Sekaran NK, Alagille D, Tamagnan GD, and Conn PJ (2005) A close structural analog of 2-methyl-6-(phenylethynyl)-pyridine acts as a neutral allosteric site ligand on metabotropic glutamate receptor subtype 5 and blocks the effects of multiple allosteric modulators. *Mol Pharmacol* **68:**1793-1802.

Rodriguez AL and Williams R (2007) Recent progress in the development of allosteric modulators of mGluR5. *Curr Opin Drug Discov Devel* **10:**715-722.

Swanson CJ, Bures M, Johnson MP, Linden AM, Monn JA, and Schoepp DD (2005) Metabotropic glutamate receptors as novel targets for anxiety and stress disorders. *Nat Rev Drug Discov* **4:**131-144.

Verkhratsky A and Kirchhoff F (2007) Glutamate-mediated neuronal-glial transmission. *J Anat* **210:**651-660.

Wierońska JM and Pilc A (2009) Metabotropic glutamate receptors in the tripartite synapse as a target for new psychotropic drugs. *Neurochem Int* **55:**85-97.

Molecular Pharmacology Fast Forward. Published on February 14, 2011 as DOI: 10.1124/mol.110.068882
This article has not been copyedited and formatted. The final version may differ from this version.

Figure Legends

Fig. 1. Saturation binding of [^{3}H]MPEP to membranes prepared from rat cortical astrocytes (**A**) or adult rat cerebral cortex (**B**). To characterize the MPEP binding site membranes were incubated with different concentrations of [^{3}H]MPEP (0.1-40 nM) in the absence (Total) or presence (NSB) of 1 μM MPEP (see *Methods*). Single representative experiments are shown, with similar data being obtained on at least two further occasions.

Fig. 2. Effects of orthosteric binding site occupancy on the specific binding of [^{3}H]MPEP in the presence of DFB, CPPHA, CDPPB or ADX47273 in membranes prepared from rat cortical astrocytes (left panels) or rat cortex (right panels). The abilities of DFB (**A**), CPPHA (**B**), CDPPB (**C**) or ADX47273 (**D**) to affect specific [^{3}H]MPEP binding was assessed in the absence and presence of quisqualate (30 μM). Data are presented as means ± SEM of 3-7 separate experiments performed in duplicate. Quantitative and statistical analyses of these data are presented in Table 1.

Fig. 3. Concentration-dependent effects of DFB (**A**), CPPHA (**B**), CDPPB (**C**) and ADX47273 (**D**) on quisqualate-stimulated [^{3}H]IP$_x$ accumulation in rat cortical astrocytes. Astrocytes were pre-incubated (10 min) with increasing concentrations of mGlu5 receptor PAMs followed by stimulation with an approx. EC_{20} quisqualate concentration (50 nM). Concentration-dependent increases in [^{3}H]IP$_x$ accumulation caused by mGlu5 receptor PAMs are shown in each panel compared to concentration-dependent [^{3}H]IP$_x$ accumulations stimulated by quisqualate alone. Data are shown as means ± SEM for 4-5 separate experiments each performed in duplicate.

Fig. 4. Displacement of specific [^{3}H]MPEP binding by mGlu5 receptor NAMs, MPEP and M-5MPEP, in membranes prepared from rat cortical astrocytes (**A**) or rat cortex (**B**). The indicated concentrations of NAMs were added to membranes immediately prior to addition of [^{3}H]MPEP (10 nM final concentration; see *Methods*). Effects of orthosteric binding site occupancy on the displacement of specific [^{3}H]MPEP binding by MPEP (**C**) and M-5MPEP

Molecular Pharmacology Fast Forward. Published on February 14, 2011 as DOI: 10.1124/mol.110.068882
This article has not been copyedited and formatted. The final version may differ from this version.

(**D**) was also investigated in rat cortex membranes. [^{3}H]MPEP binding was performed in the absence and presence of quisqualate (30 μM). Data are shown as means ± SEM of 3-6 separate experiments performed in duplicate. Quantitative and statistical analyses of these data are presented in Table 3.

Fig. 5. Concentration-dependent effects of MPEP on Ca^{2+} oscillations stimulated by glutamate, quisqualate or DHPG in rat cerebrocortical astrocytes. Representative traces showing the effects of incrementally increasing concentrations of MPEP (0.01 - 0.3 μM) on Ca^{2+} oscillations elicited by the continuous presence of glutamate (100 μM; **A**), quisqualate (10 μM; **B**) or DHPG (10 μM; **C**). Summary data are also shown for the concentration-dependent suppression of Ca^{2+} oscillations by MPEP when cells were stimulated by glutamate, quisqualate or DHPG (panel **D**). Mean pIC_{50} (M) values for inhibition of glutamate-, quisqualate- or DHPG-stimulated Ca^{2+} oscillation frequency by MPEP were 7.90 ± 0.06, 7.71 ± 0.07 and 7.82 ± 0.06, respectively. Data are shown as means ± SEM from at least 50 individual cells recorded over at least 3 separate experiments.

Fig. 6. Concentration-dependent effects of M-5MPEP on Ca^{2+} oscillation frequency stimulated by glutamate, quisqualate or DHPG in rat cerebrocortical astrocytes. Representative traces showing the effects of incrementally increasing concentrations of M-5MPEP (0.01 - 10 μM) on Ca^{2+} oscillations elicited by the continuous presence of glutamate (100 μM; **A**), quisqualate (10 μM; **B**) or DHPG (10 μM; **C**). Summary data are also shown for the concentration-dependent suppression of Ca^{2+} oscillations by M-5MPEP when cells were stimulated by glutamate, quisqualate or DHPG (panel **D**). Mean pIC_{50} (M) values for inhibition of glutamate-, quisqualate- or DHPG-stimulated Ca^{2+} oscillation frequency by M-5MPEP were 6.61 ± 0.08, 6.77 ± 0.13 and 6.38 ± 0.15, respectively. Data are shown as means ± SEM from at least 50 individual cells recorded over at least 3 separate experiments.

Fig. 7. Effects of MPEP and M-5MPEP on agonist-stimulated [^{3}H]IP_x accumulation in rat cortical astrocytes. Increasing concentrations of mGlu5 receptor NAMs were pre-incubated for 10 min prior to orthosteric agonist addition. Data are expressed as % of maximal [^{3}H]IP_x accumulation on stimulation with quisqualate (10 μM; **A**) or DHPG (10 μM; **B**). Data shown

Molecular Pharmacology Fast Forward. Published on February 14, 2011 as DOI: 10.1124/mol.110.068882
This article has not been copyedited and formatted. The final version may differ from this version.

are means ± SEM for 4-7 separate experiments performed in duplicate. Also shown are quisqualate-stimulated concentration-response curves performed in the absence or presence of 0.03, 0.1, 0.3 or 1 μM MPEP (**C**), or 1, 3, 10 or 30 μM M-5MPEP (**D**). Either MPEP or M-5MPEP was added 10 min before addition of quisqualate at the concentrations indicated. Data are shown as means ± SEM for 3 separate experiments performed in duplicate.

Molecular Pharmacology Fast Forward. Published on February 14, 2011 as DOI: 10.1124/mol.110.068882
This article has not been copyedited and formatted. The final version may differ from this version.

	pK_i			ΔpK_i (log α)	α
	control	+ quisqualate			
astrocytes					
DFB	5.28 ± 0.04	5.47 ± 0.01	*	0.19	1.5
CPPHA	6.37 ± 0.23	6.06 ± 0.00		n/d	n/d
CDPPB	5.92 ± 0.08	6.96 ± 0.06	***	1.04	11
ADX47273	5.18 ± 0.03	5.68 ± 0.06	**	0.50	3.2
rat cortex					
DFB	5.41 ± 0.05	5.49 ± 0.12		0.08	1.2
CPPHA	6.02 ± 0.08	6.23 ± 0.11		n/d	n/d
CDPPB	6.39 ± 0.12	6.97 ± 0.08	*	0.58	3.8
ADX47273	5.51 ± 0.08	5.81 ± 0.05	*	0.30	2.0

Table 1. Equilibrium dissociation constants (expressed as pK_i values) for mGlu5 receptor PAMs in the absence and presence of quisqualate (30 μM) in membranes prepared from cortical astrocytes or rat cortex. Data are shown as means ± SEM for 5-7 experiments in the absence of quisqualate and 3 experiments in the presence of quisqualate all performed in duplicate. Also shown is the shift in pK_i value in the presence and absence of quisqualate and its anti-logarithm which represents the affinity cooperativity (α) between the PAM and agonist. Statistical differences for ± quisqualate comparisons are indicated by *p<0.05; **p<0.01; ***p<0.001 (unpaired Student's t-test). n/d – value not determined for CPPHA as it is not competitive with respect to MPEP.

Molecular Pharmacology Fast Forward. Published on February 14, 2011 as DOI: 10.1124/mol.110.068882
This article has not been copyedited and formatted. The final version may differ from this version.

	modulator curve pEC_{50}	potentiation (fold increase)	affinity, pK_B	cooperativity, $\alpha.\beta$	efficacy cooperativity, β
DFB	5.38 ± 0.11	1.45 ± 0.07	5.45	2.1	1.4
CPPHA	5.73 ± 0.05	3.21 ± 0.38	5.72	4.7	n/d
CDPPB	6.24 ± 0.12	4.55 ± 0.36	6.27	25	2.3
ADX47273	5.54 ± 0.10	4.71 ± 0.66	5.52	30	9.4

Table 2. Potency and maximal response indices for potentiation by mGlu5 receptor PAMs of $[^3H]IP_x$ accumulations stimulated by an EC_{20} concentration (50 nM) of the orthosteric agonist quisqualate in astrocytes. pEC_{50} values are given as –log (M) values, and maximum potentiation values are given as a fold increase in $[^3H]IP_x$ accumulation compared the response stimulated in the presence of 50 nM quisqualate alone. Data are shown as means ± SEM for 4-5 separate experiments each performed in duplicate. Also shown are equilibrium dissociation constants (pK_B) and net cooperativity ($\alpha.\beta$) with respect to quisqualate; the efficacy cooperativity (β) is estimated by dividing the overall cooperativity ($\alpha.\beta$) by the affinity cooperativity (α; Table 1).

Molecular Pharmacology Fast Forward. Published on February 14, 2011 as DOI: 10.1124/mol.110.068882
This article has not been copyedited and formatted. The final version may differ from this version.

	control	+ quisqualate (30 μM)
astrocytes		
MPEP	8.03 ± 0.06 (n=3)	-
M-5MPEP	6.18 ± 0.04 (n=3)	-
5MPEP	6.03 ± 0.09 (n=3)	-
rat cortex		
MPEP	8.18 ± 0.06 (n=6)	8.18 ± 0.09 (n=3)
M-5MPEP	6.57 ± 0.06 (n=6)	6.70 ± 0.02 (n=3)
5MPEP	6.48 ± 0.06 (n=6)	6.64 ± 0.01 (n=3)

Table 3. Comparison of binding affinity constants (expressed as $-\log K_i$ (pK_i) values) for mGlu5 receptor NAMs in the absence and presence of quisqualate (30 μM) in astrocyte and rat cortex membranes. There were no statistical differences between control and quisqualate-treated rat cortex membranes as determined by unpaired Student's *t*-test.

Molecular Pharmacology Fast Forward. Published on February 14, 2011 as DOI: 10.1124/mol.110.068882
This article has not been copyedited and formatted. The final version may differ from this version.

orthosteric agonist	NAM	[^{3}H]IP$_x$			Ca^{2+} oscillations		
		pIC_{50} (M)	% max. inhibition	*n*	pIC_{50} (M)	% max. inhibition	*n*
glutamate	MPEP	-	-	-	7.90 ± 0.06	99.9 ± 4.6	3
	M-5MPEP	-	-	-	6.61 ± 0.08	94.8 ± 9.8	5
quisqualate	MPEP	7.77 ± 0.03	90.0 ± 1.9	4	7.71 ± 0.07	97.0 ± 5.1	3
	M-5MPEP	5.55 ± 0.04	40.3 ± 4.1	7	6.77 ± 0.13	103.6 ± 7.2	3
DHPG	MPEP	7.15 ± 0.08	97.0 ± 2.3	4	7.82 ± 0.06	100.7 ± 4.6	3
	M-5MPEP	5.66 ± 0.01	52.6 ± 4.1	4	6.38 ± 0.15	101.6 ± 5.2	3

Table 4. Comparison of potency (pIC_{50}) and efficacy (R_{max}) indices for mGlu5 receptor-mediated [^{3}H]IP$_x$ and Ca^{2+} responses. pEC_{50} values are given as –log M values, and R_{max} values are given as a percentage of the maximal response to quisqualate.

A.

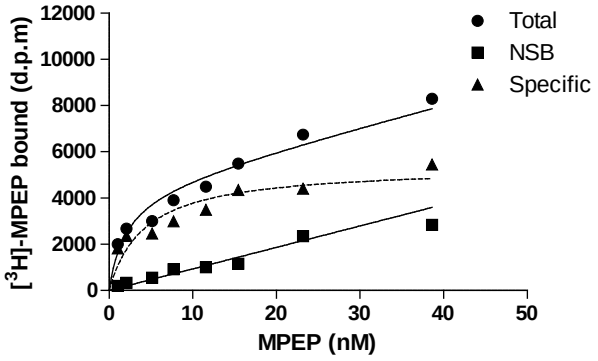
12000
10000
8000
6000
4000
2000
0
[3H]-MPEP bound (d.p.m)
0
10
20
30
40
50
MPEP (nM)
Total
NSB
Specific

B.

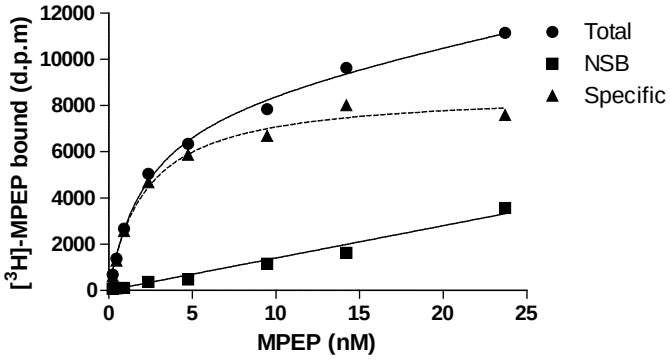
12000
10000
8000
6000
4000
2000
0
[3H]-MPEP bound (d.p.m)
0
5
10
15
20
25
MPEP (nM)
Total
NSB
Specific

A.

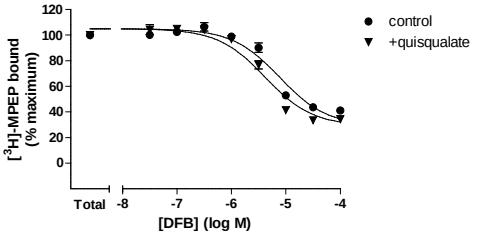
[^{3}H]-MPEP bound (% maximum)
120
100
80
60
40
20
0
Total
-8
-7
-6
-5
-4
[DFB] (log M)
control
+quisqualate

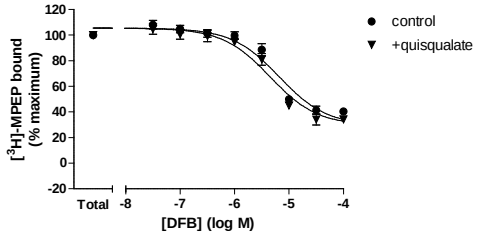
[^{3}H]-MPEP bound (% maximum)
120
100
80
60
40
20
0
-20
Total
-8
-7
-6
-5
-4
[DFB] (log M)
control
+quisqualate

B.

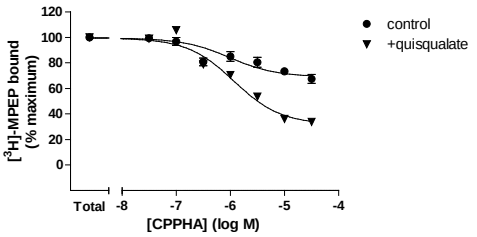
[^{3}H]-MPEP bound (% maximum)
120
100
80
60
40
20
0
Total
-8
-7
-6
-5
-4
[CPPHA] (log M)
control
+quisqualate

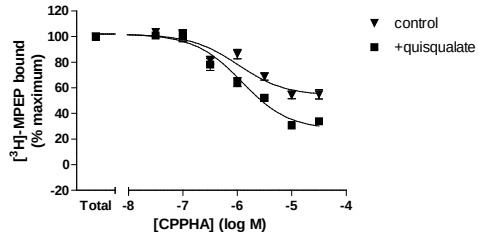
[^{3}H]-MPEP bound (% maximum)
120
100
80
60
40
20
0
-20
Total
-8
-7
-6
-5
-4
[CPPHA] (log M)
control
+quisqualate

C.

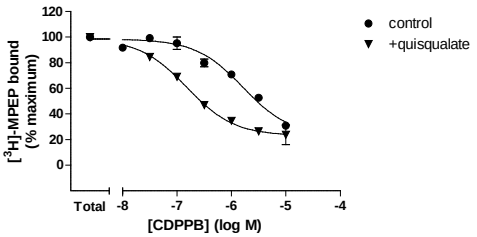
[^{3}H]-MPEP bound (% maximum)
120
100
80
60
40
20
0
Total
-8
-7
-6
-5
-4
[CDPPB] (log M)
control
+quisqualate

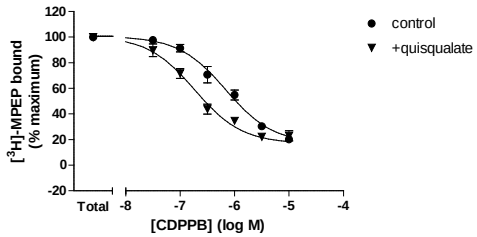
[^{3}H]-MPEP bound (% maximum)
120
100
80
60
40
20
0
-20
Total
-8
-7
-6
-5
-4
[CDPPB] (log M)
control
+quisqualate

D.

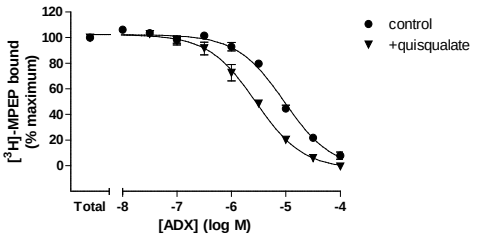
[^{3}H]-MPEP bound (% maximum)
120
100
80
60
40
20
0
Total
-8
-7
-6
-5
-4
[ADX] (log M)
control
+quisqualate

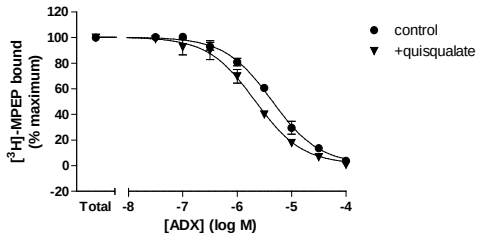
[^{3}H]-MPEP bound (% maximum)
120
100
80
60
40
20
0
-20
Total
-8
-7
-6
-5
-4
[ADX] (log M)
control
+quisqualate

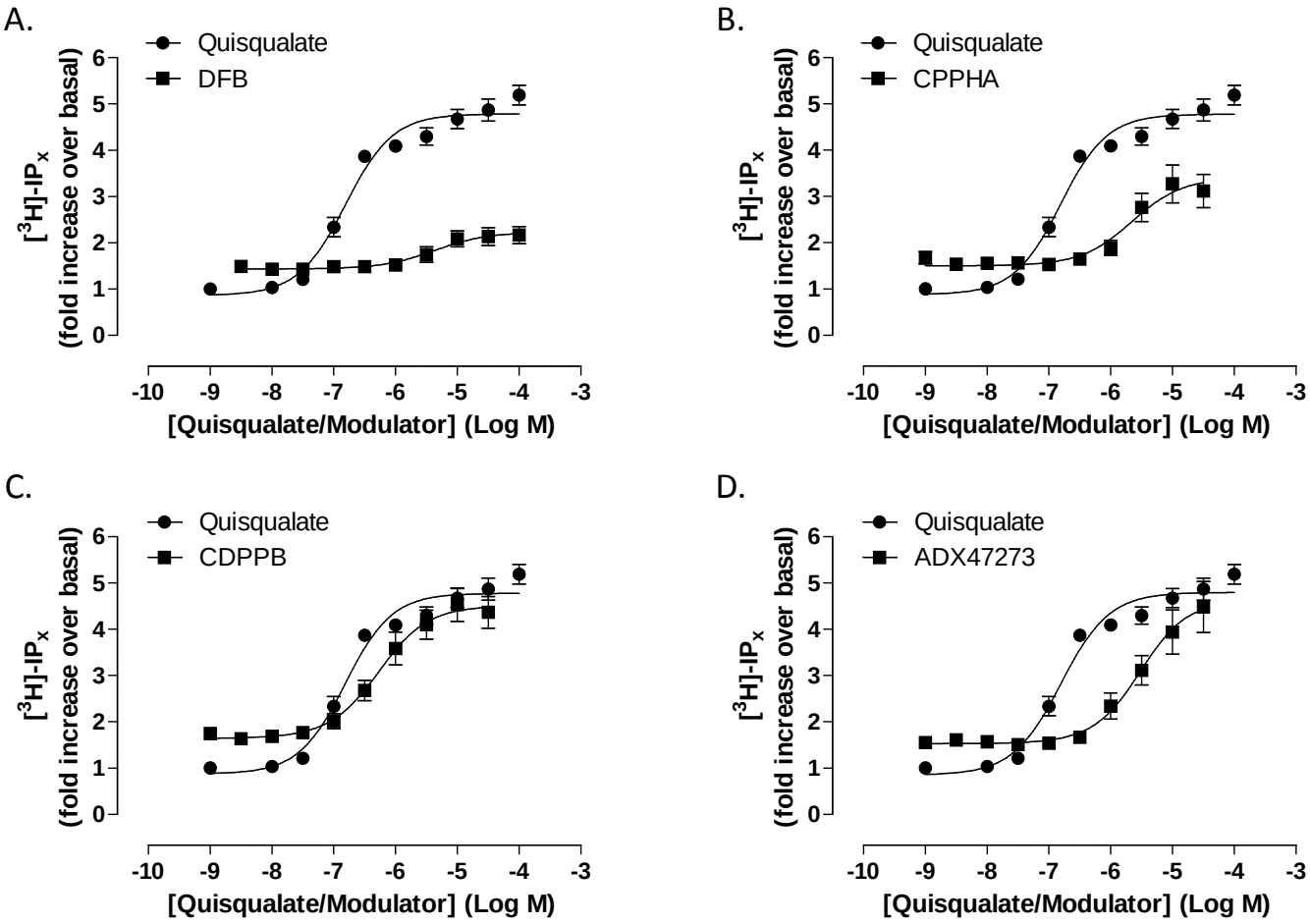
A.
Quisqualate
DFB
[3H]-IPx
(fold increase over basal)
[Quisqualate/Modulator] (Log M)
B.
Quisqualate
CPPHA
[3H]-IPx
(fold increase over basal)
[Quisqualate/Modulator] (Log M)
C.
Quisqualate
CDPPB
[3H]-IPx
(fold increase over basal)
[Quisqualate/Modulator] (Log M)
D.
Quisqualate
ADX47273
[3H]-IPx
(fold increase over basal)
[Quisqualate/Modulator] (Log M)

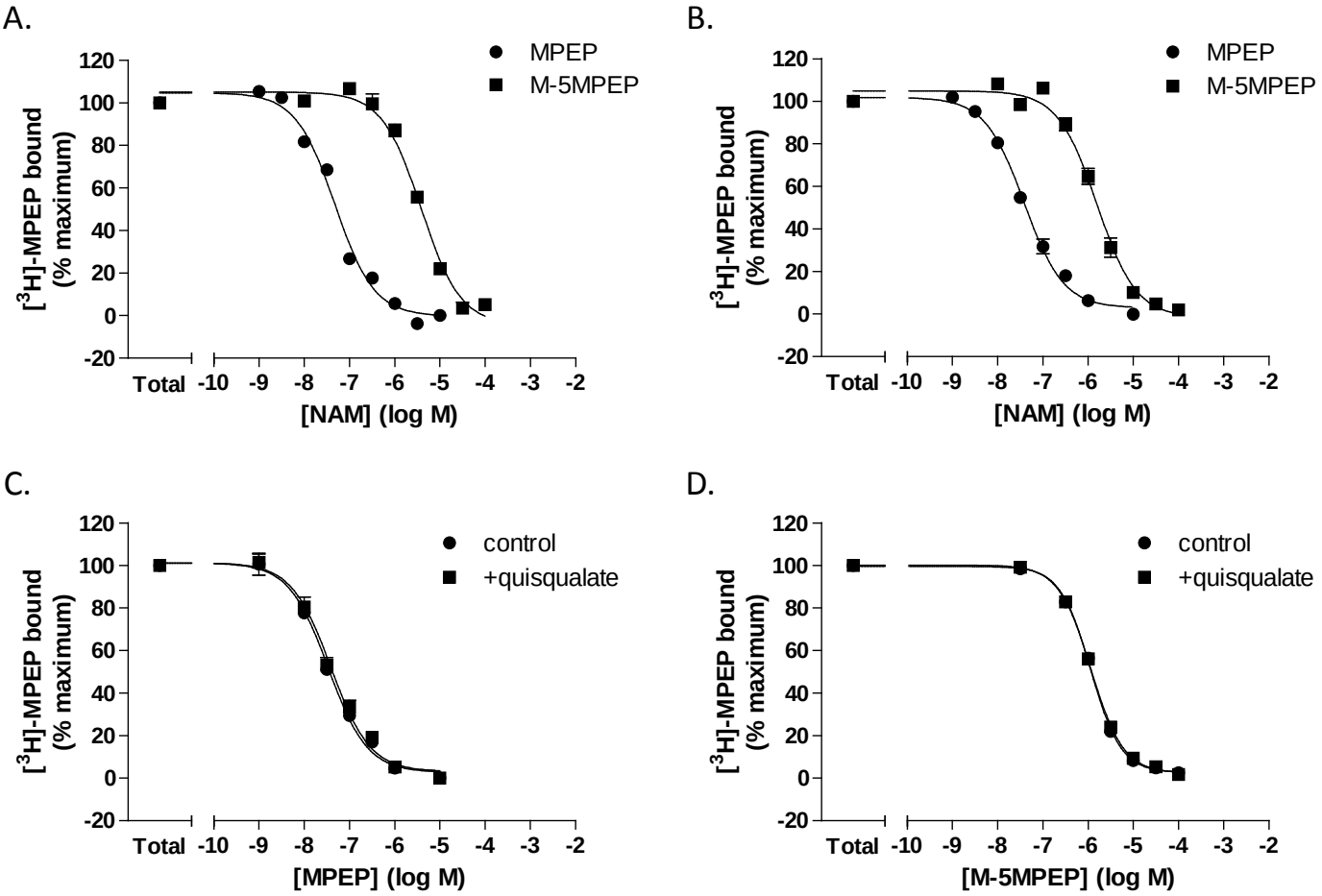
A.
MPEP
M-5MPEP
[3H]-MPEP bound (% maximum)
120
100
80
60
40
20
0
-20
Total
-10
-9
-8
-7
-6
-5
-4
-3
-2
[NAM] (log M)
B.
MPEP
M-5MPEP
[3H]-MPEP bound (% maximum)
[NAM] (log M)
C.
control
+quisqualate
[3H]-MPEP bound (% maximum)
[MPEP] (log M)
D.
control
+quisqualate
[3H]-MPEP bound (% maximum)
[M-5MPEP] (log M)

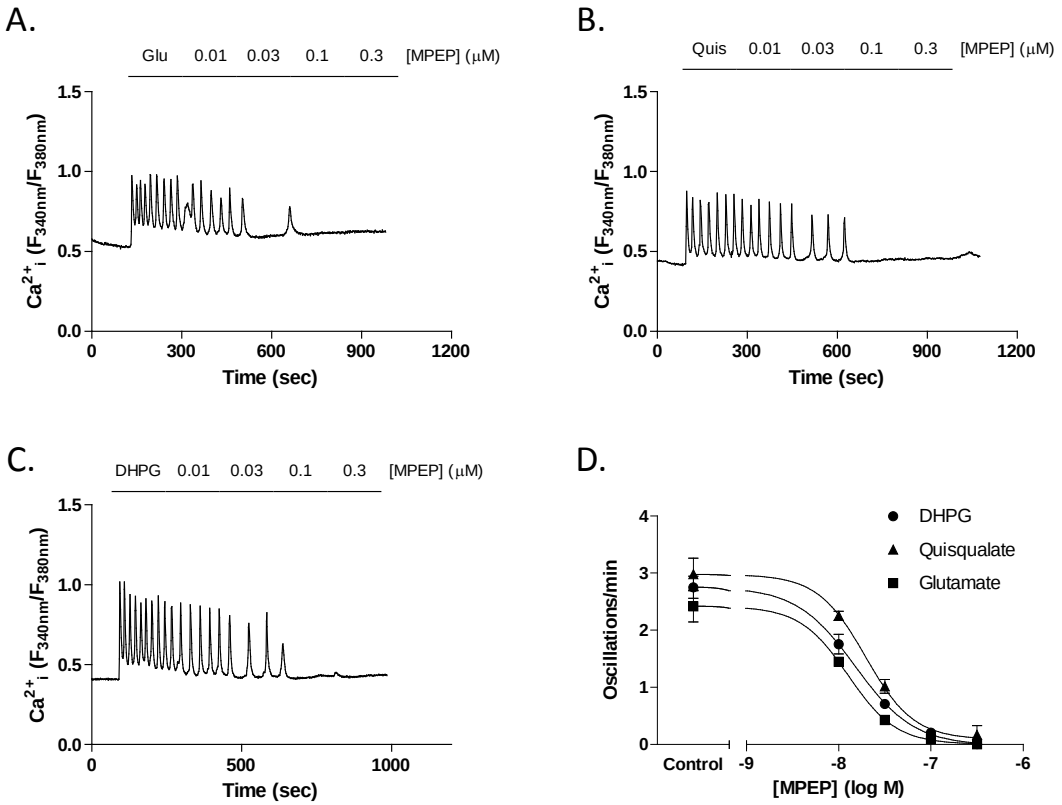
A.
Glu 0.01 0.03 0.1 0.3 [MPEP] (μM)
Ca2+ i (F340nm/F380nm)
1.5
1.0
0.5
0.0
0 300 600 900 1200
Time (sec)
B.
Quis 0.01 0.03 0.1 0.3 [MPEP] (μM)
Ca2+ i (F340nm/F380nm)
1.5
1.0
0.5
0.0
0 300 600 900 1200
Time (sec)
C.
DHPG 0.01 0.03 0.1 0.3 [MPEP] (μM)
Ca2+ i (F340nm/F380nm)
1.5
1.0
0.5
0.0
0 500 1000
Time (sec)
D.
DHPG
Quisqualate
Glutamate
Oscillations/min
4
3
2
1
0
Control -9 -8 -7 -6
[MPEP] (log M)

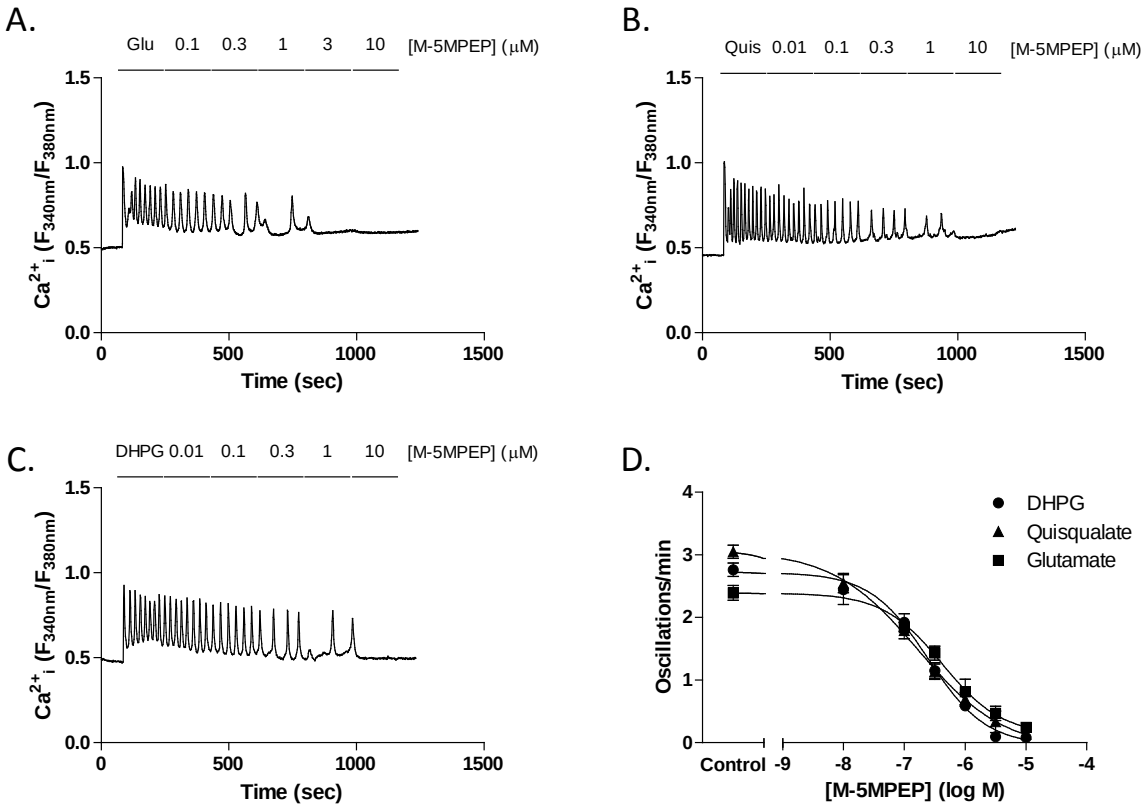
A.
Glu 0.1 0.3 1 3 10 [M-5MPEP] (μM)
Ca2+ i (F340nm/F380nm)
Time (sec)
B.
Quis 0.01 0.1 0.3 1 10 [M-5MPEP] (μM)
Ca2+ i (F340nm/F380nm)
Time (sec)
C.
DHPG 0.01 0.1 0.3 1 10 [M-5MPEP] (μM)
Ca2+ i (F340nm/F380nm)
Time (sec)
D.
DHPG
Quisqualate
Glutamate
Oscillations/min
Control
[M-5MPEP] (log M)

A.

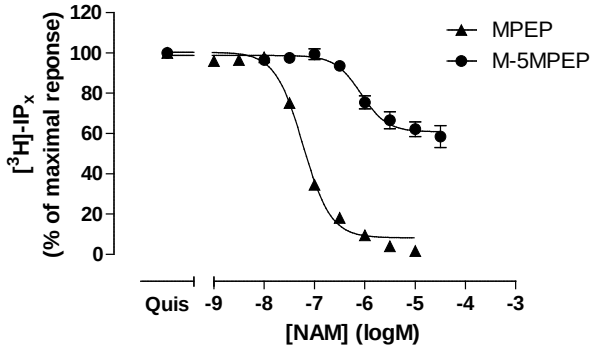
MPEP
M-5MPEP
[3H]-IPx
(% of maximal reponse)
120
100
80
60
40
20
0
Quis
-9
-8
-7
-6
-5
-4
-3
[NAM] (logM)

B.

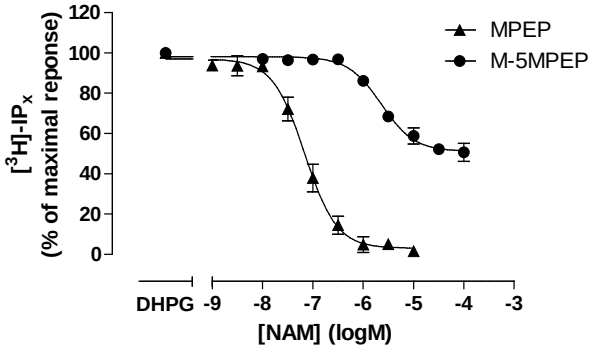
MPEP
M-5MPEP
[3H]-IPx
(% of maximal reponse)
120
100
80
60
40
20
0
DHPG
-9
-8
-7
-6
-5
-4
-3
[NAM] (logM)

C.

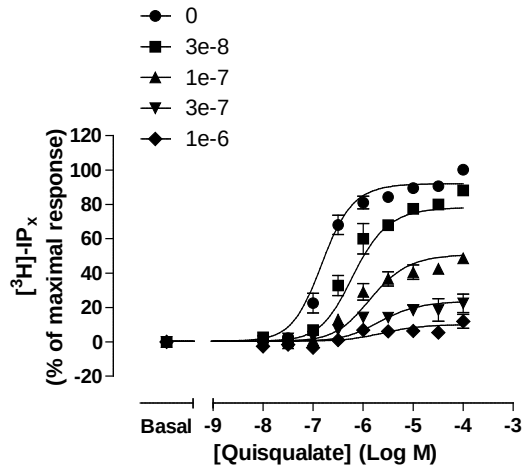
0
3e-8
1e-7
3e-7
1e-6
[3H]-IPx
(% of maximal response)
120
100
80
60
40
20
0
-20
Basal
-9
-8
-7
-6
-5
-4
-3
[Quisqualate] (Log M)

D.

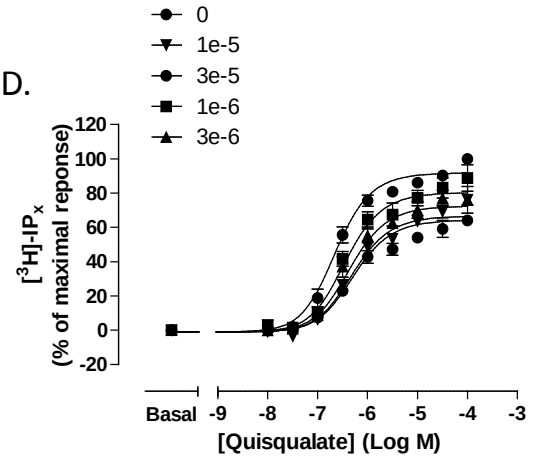
0
1e-5
3e-5
1e-6
3e-6
[3H]-IPx
(% of maximal reponse)
120
100
80
60
40
20
0
-20
Basal
-9
-8
-7
-6
-5
-4
-3
[Quisqualate] (Log M)